Tube-based Distributed Model Predictive Control for Heterogeneous Vehicle Platoons via Convex Optimization

Hao Sun, Li Dai and Boli Chen

***Abstract*— Connected and autonomous driving technology is a current research hotspot, which can effectively ease transportation congestion and enhance road safety. This paper addresses the control problem of heterogeneous vehicle platoons subject to various disturbances, including but not limited to modeling and measurement disturbances. The problem is approached by a tube-based distributed model predictive control (MPC) algorithm that relies on a unidirectional predecessor-following communication topology. To improve the computational efficiency of the algorithm, the inherently nonlinear MPC problem is formulated as a convex program in the spatial domain by coordination changes and suitably relaxing the nonconvex constraints. Numerical simulation examples are carried out to show the effectiveness and robustness of the proposed control algorithm.**

I. Introduction

The rollout of connected and autonomous vehicles (CAVs) with enhanced electrification and digitisation is predicted to alleviate the traffic congestion safety issues by delivering a wide range of environmental, social and economic benefits. To maximize the benefit of CAV technologies, cooperative CAV control has received increasing attention in the past decades. One of the most important applications of cooperative CAV control technologies is vehicle platooning. In principle, a cooperative controller takes advantage of vehicle-to-everything (V2X) communications (V2V, V2I) to allow CAVs to form platoons and be driven at harmonised speeds with reduced time/distance headways between them.

The work on platoon control can be traced back to the Program on Advanced Technology for the Highway (PATH) [1] at the University of California, Berkeley in the 1980s. Since then, many industries and research organizations have developed and tested this technology. For example, the EU launched Safe Road Trains for the Environment (SARTRE) [2] in 2009, Peloton Technology Inc. in America released a new L4 level automated following strategy [3] in 2019.

Existing literature on vehicle platooning focus mainly on longitudinal control [4]–[13]. In these studies, different control methods, including model predictive control (MPC) [12], consensus-based control [9], fuzzy control [7], and sliding-mode control [13], have been applied to address string stability of the platoon, which is one of the fundamental problems. Early studies use double-integrator vehicle models, which simplify the analysis and control design at the price of sacrificed accuracy [14]. Moreover, the double-integrator model limits application scope to homogeneous platoons only, which is not the case in practice. This calls for research on heterogeneous platoon control, where the heterogeneity stems from differences in powertrain components and body parameters. The distributed MPC represents a typical solution, which incorporates heterogeneity in controller design [15]–[17]. Dynamical heterogeneity can also be thought of as restricted uncertainty imposed on homogeneous platoon framework, allowing for robust control [18], [19]. Due to the nonlinearity entailed in the vehicle dynamics, the MPC based approaches usually involve time-consuming nonlinear optimization, which impedes their application in real-time.

Despite the vast literature on platoon control, uncertainties and disturbances are not considered in the majority of works. Recently, to address various uncertainties appearing in the platoon systems, several robust algorithms have been developed. A tube-based robust MPC approach is proposed in [17] with consideration of process noise. A sliding mode control method is proposed in [13], where uncertain communication topologies are addressed. Moreover, communication delays are coped with in [20]. Nevertheless, there is still a lack of heterogeneous platoon control strategy that can address multiple disturbances within a single framework.

In this paper, a novel platoon control algorithm is proposed to achieve a heterogeneous vehicle platoon control in the longitudinal direction through predecessor-following (PF) communication topology. Process disturbances and measurement noises are taken into consideration from multiple sources. Specific contributions can be summarized as follows:

- With proper relaxation of the nonlinearities stemming from the vehicle dynamics, a convex framework of the heterogeneous platoon control problem is established in the space domain, which enables a fast and unique control solution.
- In contrast to the existing robust platoon control methods that focus only on the process noise, this paper addressed process and measurement disturbances based on a tube-based MPC strategy.

The rest of this paper is organized as follows. In Section II, the platoon control problem is introduced. In Section III, a tube-based robust MPC algorithm is designed to deal with robust platoon control problem. Simulation results are illustrated and discussed in Section IV. Finally, Section V draws the conclusion of the work.

Notation: Let $\mathbb{R}$, $\mathbb{R}_{\geq 0}$, $\mathbb{R}_{>0}$ and $\mathbb{N}_{>0}$ denote the real, the non-negative real, the strict positive real sets of numbers and non-zero natural numbers, respectively. Given a vector $\mathbf{x} \in \mathbb{R}^n$, we will denote as $|\mathbf{x}|$ the Euclidean norm of $\mathbf{x}$. Given a

H. Sun and B. Chen are with the Department of Electronic and Electrical Engineering, University College London, UK, WC1E 6BT (h.sun.20@ucl.ac.uk; boli.chen@ucl.ac.uk).

L. Dai is with the School of Automation, Beijing Institute of Technology, Beijing 100081, China (daili1887@gmail.com).

This work has been partially supported by The Royal Society International Exchanges programme, IES\R2\212041.

time-varying vector $\mathbf{x}(t) \in \mathbb{R}^n$, $t \in \mathbb{R}_{\geq 0}$ we will denote as $\|\mathbf{x}\|_\infty$ the quantity $\|\mathbf{x}\|_\infty = \sup_{t\geq 0}|\mathbf{x}(t)|$. Given a matrix $\mathbf{A} \in \mathbb{R}^{n\times n}$, then $||\mathbf{A}||$ will denote $\max_{\mathbf{x}\in\mathbb{R}^n\setminus 0}\{|\mathbf{A}\mathbf{x}|/|\mathbf{x}|\}$. For a vector $x \in \mathbb{R}^n$ and a positive semi-definite matrix $Q \in \mathbb{R}^{n\times n}$, $||x||_Q = (x^\top Q x)^{1/2}$ denotes the weighted Euclidean norm of x.

The Minkowski sum of sets $\mathbb{W}, \mathbb{V}$ is $\mathbb{W} \oplus \mathbb{V} = \{\ x + y \mid x \in \mathbb{W}, y \in \mathbb{V}\ \}$; the Minkowski difference of sets $\mathbb{W}, \mathbb{V}$ is $\mathbb{W} \ominus \mathbb{V} = \{\ x \mid x \oplus \mathbb{V} \subseteq \mathbb{W}\ \}$.

II. Problem Statement

A. Platoon Model for Control

This paper considers the longitudinal control of a heterogeneous vehicle platoon with a PF communication topology on a level road with $N+1$ CAVs, including a leading vehicle (indexed by 0) and N following CAVs (indexed from 1 to N) as illustrated in Fig. 1. This communication scheme is

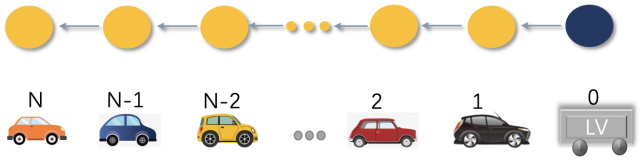

Fig. 1. PF communication topology: each vehicle only receives information from the front one

unidirectional between each two consecutive vehicles, which is commonly used in the field of vehicle platoon [21], [22].

The longitudinal dynamics of the ith vehicle described as

$$\dot{s}_i(t) = v_i(t) \tag{1a}$$
$$\dot{v}_i(t) = \frac{1}{m_i}\left(\frac{\eta_i}{r_i}T_i(t) - C_{d,i}v_i^2(t) + m_i g f_i\right),\ i \in \mathcal{N} \tag{1b}$$

where $\mathcal{N} = \{1, 2, \cdots, N\}$ is the set of all following vehicles, $s_i(k)$ and $v_i(k)$ are the position and velocity of the vehicle i, m_i is the vehicle mass; η_i is the final drive ratio, r_i is the tire radius, $C_{d,i}$ is the coefficient of aerodynamic drag, g is the gravity constant, f_i is the coefficient of rolling resistance, and T_i is the driving/braking torque.

In order to strike the balance between control performance and computational efficiency, the convex relaxation approach proposed in the authors' previous work [23] is adopted. The key idea is to turn the problem into space domain with suitable state transformations. Let s denote the variable of traveled distance. By changing the independent variable t to s by $\frac{d}{ds} = \frac{1}{v}\frac{d}{dt}$, the longitudinal dynamics can be rewritten as:

$$\frac{d}{ds}t_i(s) = \zeta_i(s), \tag{2a}$$
$$\frac{d}{ds}E_i(s) = \frac{\eta_i}{r_i}T_i(s) - 2\frac{C_{d,i}}{m_i}E_i(s) - m_i g f_i \tag{2b}$$
$$\zeta_i(s) \geq \frac{1}{\sqrt{2E_i(s)/m_i}} \tag{2c}$$

where $t_i(s)$ and $E_i(s)$ are the time and kinetic energy consumption of vehicle i, respectively. Moreover, $\zeta_i(s)$ is the auxiliary control variable to linearize the nonlinear dynamics of t_i.

To avoid coupled state constraints with regard to the headways between consecutive vehicles, it is reasonable to reformat the system (2) as follow to avoid coupled state constraints

$$\frac{d}{ds}\Delta t_i(s) = \zeta_i(s) - \frac{1}{v_{i-1}(s)} \tag{3a}$$
$$\frac{d}{ds}\Delta E_i(s) = \frac{\eta_i}{r_i}T_i(s) - 2\frac{C_{d,i}}{m_i}E_i(s) - m_i g f_i - \kappa_{i-1}(s) \tag{3b}$$

where (2c) remains, $\Delta t_i(s) = t_i(s) - t_{i-1}(s)$ and $\Delta E_i(s) = E_i(s) - E_{i-1}(s)$ are the time headway and kinetic energy difference between vehicle i and the preceding vehicle $i-1$, $v_{i-1}(s)$ is the velocity of the preceding vehicle and $\kappa_{i-1}(s) = \frac{d}{ds}E_{i-1}(s)$ are the total force acting on the wheels of vehicle $i-1$.

III. Tube-based Distributed Control Algorithm

Prior to the introduction of the MPC algorithm, let us first introduce the system model in a discretized form of (3). Let $\Delta s \in \mathbb{R}_{>0}$ be the sampling distance interval and assume that the trip length equals to $\bar{k}\Delta s$, $\bar{k} \in \mathbb{N}_{>0}$. Considering $x_i = [\Delta t_i\ \Delta E_i]^\top$ and $u_i = [\zeta_i\ T_i]^\top$, the discretized system dynamics of (3) are given by:

$$\begin{aligned} x_i(k+1) &= A_i x_i(k) + B_i u_i(k) + \gamma_i(t) + d_i(k) \\ y_i(k) &= C x_i(k) + w_i(k), i \in \mathcal{N} \end{aligned} \tag{4}$$

$$A_i = \begin{bmatrix} 1 & 0 \\ 0 & 1 - \frac{2C_{d,i}}{m_i}\Delta s \end{bmatrix},\ B_i = \begin{bmatrix} \Delta s & 0 \\ 0 & \frac{\eta_i}{r_i}\Delta s \end{bmatrix},\ C = \begin{bmatrix} 1 & 0 \\ 0 & 1 \end{bmatrix},$$
$$\gamma_i(k) = \begin{bmatrix} -\frac{\Delta s}{v_{i-1}(k)} \\ \Delta s\left(-2\frac{C_{d,i}}{m_i}E_{i-1}(k) - m_i g f_i - \kappa_{i-1}(k)\right) \end{bmatrix}$$

where $k = 0, 1, \ldots, \bar{k}$, y_i is the measurement of the Δt_i and ΔE_i obtained by the ith vehicle's onboard sensors (*e.g.*, front radar and speedometer). γ_i embodies $v_{i-1}(k)$, $E_{i-1}(k)$, $\kappa_{i-1}(k)$ of the $i-1$th vehicle, which are all known to vehicle i at step k (from the onboard sensors of the ith vehicle). $d_i(k) \in \mathbb{D}_i$ and $w_i(k) \in \mathbb{W}_i$ respectively represent the process noise and measurement noise with $\mathbb{D}_i = \{d_i(k) \in \mathbb{R}^2 : ||d_i(k)||_\infty \leq \bar{d}_i\}, \bar{d}_i \in \mathbb{R}_{>0}$ and $\mathbb{W}_i = \{w_i(k) \in \mathbb{R}^2 : ||w_i(k)||_\infty \leq \bar{w}_i\}, \bar{w}_i \in \mathbb{R}_{>0}$, are closed convex sets with bounds on d_i and w_i, respectively. Furthermore, the control inputs and the system states are subject to the constraints

$$x_i \in \mathbb{X}_i, \qquad u_i \in \mathbb{U}_i \tag{5}$$

due to the physical limits and safety requirements.

On the other hand, the nominal system is defined, which will be instrumental for the upcoming analysis:

$$\bar{x}_i(k+1) = A_i\bar{x}_i(k) + B_i\bar{u}_i(k) + \gamma_i(k) \tag{6}$$

where the disturbances d_i and w_i are neglected, $\bar{x}_i(k) = [\Delta\bar{E}_i, \Delta\bar{t}_i]$ is the nominal state, and $\bar{u}_i(k)$ is the nominal

control input and the nominal output is identical to the state: $\bar{y}_i(k) = \bar{x}_i(k)$ provided C an identity matrix.

The objective of the platoon control is to track the speed of the leader vehicle while maintaining a desired constant time headway (equivalent to a constant distance gap when the speed of leader is constant in steady state) between any consecutive vehicles

$$\lim_{k\to\infty} ||v_i(k) - v_0|| = 0 \tag{7a}$$
$$\lim_{k\to\infty} ||t_i(k) - t_{i-1}(k) - \delta|| = 0,\ \forall i \in \mathcal{N} \tag{7b}$$

where v_0 is the target (steady-state) velocity of the leading vehicle, δ is the desired time gap between consecutive vehicles. With the system states Δt_i and ΔE_i defined in (4), the objective given in (7) can be reformatted as follows

$$\lim_{k\to\infty} ||E_i(k) - E_0(k)|| = \frac{1}{2}|m_i - m_0|v_0^2(k) \tag{8a}$$
$$\lim_{k\to\infty} ||\Delta t_i(k) - \delta|| = 0,\ \forall i \in \mathcal{N} \tag{8b}$$

A. Tube-based MPC

In this subsection, the tube-based robust MPC algorithm [24], [25] is introduced. To deal with the measurement noise, a Luenberger observer is designed for system (4):

$$\begin{aligned}\hat{x}_i(k+1) &= A_i\hat{x}_i(k) + B_iu_i(k) + \gamma_i(t) + L_i(y_i(k) - \hat{y}_i(k))\\ \hat{y}_i(k) &= C\hat{x}_i(k)\end{aligned} \tag{9}$$

where $\hat{x}_i$ is the estimate of the state, L_i is the observer gain, such that the spectral radius of $A_i - L_iC$ satisfies the condition $\rho(A_i - L_iC) < 1$. Consider the error $\tilde{x}_i = x_i - \hat{x}_i$, the dynamics of which are governed by

$$\tilde{x}_i(k+1) = (A_i - L_iC)\tilde{x}_i(k) + (d_i(s) - L_iw_i(k)) \tag{10}$$

It can be inferred from (10) that $d_i(k) - L_iw_i(k)$ is bounded by a set $\tilde{\Delta}_i$, defined as:

$$\tilde{\Delta}_i = \mathbb{D}_i \oplus (-L_i\mathbb{W}_i) \tag{11}$$

Therefore, the minimal robust invariant set $\tilde{\mathbb{S}}_i$ associated with $\tilde{x}$ can be obtained:

$$\tilde{\mathbb{S}}_i = \oplus_{k=0}^{\infty}(A_i - L_iC)^k\tilde{\Delta}_i \tag{12}$$

The robust control policy is formed by an open-loop control solved by an optimization problem with nominal dynamics (6) and tightened constraints, and an ancillary feedback control based on the state estimation. The feedback controller is defined as:

$$u_i(k) = \bar{u}_i(k) + K_ie_i(k) \tag{13}$$

where K_i is the gain of the feedback controller such that $A_i + B_iK_i$ meets the condition $\rho(A_i + B_iK_i) < 1$. e_i is the tracking error between the observer state and the nominal system, $e_i(k)$ is described by:

$$e_i(k) = \hat{x}_i(k) - \bar{x}_i(k) \tag{14}$$

Combined with equation (9), we obtain

$$\begin{aligned}\tilde{x}_i(k+1) = A\hat{x}_i(k) + B_i\bar{u}_i(k) + B_iK_ie_i(k)\\ + L_iC\tilde{x}_i(k) + L_iw_i(k)\end{aligned} \tag{15}$$

Then, it is immediate to show that

$$e_i(k+1) = (A_i + B_iK_i)e_i(k) + (L_iC\tilde{x}_i(k) + L_iw_i(k)) \tag{16}$$

Therefore, $L_iC\tilde{x}_i(k) + L_iw_i(k)$ can be bounded by:

$$\overline{\Delta}_i = L_iC\tilde{\mathbb{S}}_i \oplus L_i\mathbb{W}_i \tag{17}$$

Therefore, the minimal robust invariant set $\tilde{\mathbb{S}}_i$ for e_i is obtained:

$$\overline{\mathbb{S}}_i = \oplus_{k=0}^{\infty}(A_i + B_iK_i)^k\overline{\Delta}_i \tag{18}$$

To ensure that the state and control constraints are not violated in the disturbed scenario, the following tightened constraints have to be utilized in the MPC algorithm (see (20)) rather than the constrains (5):

$$\begin{aligned}\bar{x}_i &\in \mathbb{X}_i \ominus (\tilde{\mathbb{S}}_i \oplus \overline{\mathbb{S}}_i)\\ \bar{u}_i &\in \mathbb{U}_i \ominus K_i\overline{\mathbb{S}}_i\end{aligned} \tag{19}$$

The detailed formulation of the MPC problem will be shown in the next Section III-B.

B. Distributed MPC algorithm

To introduce the distributed MPC framework, let us denote by N_p the prediction horizon used in all local control problems. Over any horizon $[k+0, k+N_p-1]$, $k = 1, 2, \cdots, \bar{k}$, we define two types of trajectories, which are instrumental for constructing the distributed MPC framework:

- Optimal state trajectory $x_i^*(j|k)$
- Assumed state trajectory $x_i^a(j|k)$

where $j \in [0, N_p - 1]$. Similarly, the assumed control input u_i^a and the optimal control input u_i^* are defined. More specifically, $x_i^*(j|k) = [\Delta t_i^*(j|k)\ \Delta E_i^*(j|k)]^\top$ is the optimal solution after numerically solving the local MPC problem and $x_i^a(j|k) = [\Delta t_i^a(j|k)\ \Delta E_i^a(j|k)]^\top$ is the assumed trajectory transmitted from vehicle i to $i+1$ together with the assumed energy $E_i^a(j|k)$ and the assumed total force $\kappa_i^a(j|k)$. In particular, $E_i^a(j|k)$ is obtained by $E_i^a(j|k) = E_{i-1}^a(j|k) + \Delta E_i^a(j|k), \forall i \in \mathcal{N}$ with $E_0^a(j|k) = E_0(k)$ and $\kappa_i^a(j|k) = (E_i^a(j|k) - E_i^a(j|k-1))/\Delta s$, which are utilized to construct the assumed signal $\gamma_i^a(j|k)$. When $k = 0$, $x_i^a(j|0) = x_i(0), \forall j \in [0, N_p - 1]$ and when $k > 0$, $x_i^a(j|k)$ is constructed by using the optimal state trajectory obtained in the previous step, $x_i^*(j|k-1)$. In Fig 2, the relationships between optimal trajectory and assumed trajectory are demonstrated. As it can be seen, the $k+1$ step

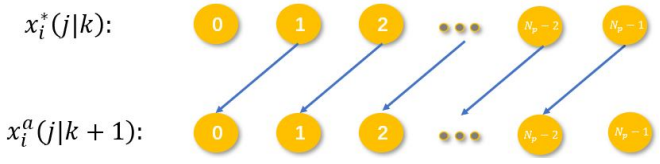

Fig. 2. Relationships between x_i^* and x_i^a

assumed state trajectory is determined by $x_i^a(j|k+1) = x_i^*(j+1|k), \forall j \in [0, N_p - 2]$ and $x_i^a(N_p - 1|k+1) = A_ix_i^a(N_p - 2|k+1) + B_iu_i^a(N_p - 2|k+1) + \gamma_i^a(N_p - 1|k)$, where $u_i^*(N_p - 1|k)$ is constructed by assuming that the

acceleration of ith vehicle is 0 (counterbalance the all friction losses):

$$u_i^*(N_p-1|k) = \begin{bmatrix} 1/\sqrt{2(\Delta E_i^*(N_p-1|k)+E_{i-1}^a(N_p-1|k))/m_i} \\ \frac{r_i}{\eta_i}\left(\frac{2C_{d,i}}{m_i}(\Delta E_i^*((N_p-1|k)+E_{i-1}^a((N_p-1|k)) + m_i g f_i\right) \end{bmatrix}$$

By analogy to the assumed state trajectory, assumed control trajectory $u_i^a(j|k+1) = u_i^*(j+1|k)$, $\forall j \in [0, N_p-2]$.

To achieve the control objective defined in (8), the local optimal control problem for each CAV i is designed as *Problem*:

$$\min_{\bar{u}_i} \; J_i(k) = \sum_{j=0}^{N_p-1} l_i(\bar{x}_i(j|k), \bar{u}_i(j|k), x_i^a(j|k)) \tag{20a}$$

s.t.

$$\bar{x}_i(j+1|k) = A_i(\bar{x}_i(j|k)) + B_i\bar{u}_i(j|k) + \gamma_i^a(j|k) \tag{20b}$$

$$\bar{x}_i(j|k) \in \mathbb{X}_i \ominus (\tilde{\mathbb{S}}_i \oplus \bar{\mathbb{S}}_i) \tag{20c}$$

$$\bar{u}_i(j|k) \in \mathbb{U}_i \ominus K_i\bar{\mathbb{S}}_i \tag{20d}$$

$$\bar{\zeta}_i(j|k) \geq \frac{1}{\sqrt{(\Delta E_i(j|k) + E_{i-1}^a(j|k))/m_i}} \tag{20e}$$

$$\bar{x}_i(0|k) = x_i(k) \tag{20f}$$

where J_i is the cost function associated with vehicle i, defined as

$$\begin{aligned} &l_i(\bar{x}_i(j|k), \bar{u}_i(j|k), x_i^a(j|k)) \\ &\quad = ||\bar{T}_i(j|k) - h_i(j|k)||_{R_i}^2 + ||\bar{x}_i(j|k) - x_i^a(j|k)||_{F_i}^2 \\ &\quad + ||\bar{x}_i(j|k) - x_{des,i}(j|k)||_{G_i}^2 + ||\bar{\zeta}_i(j|k)\Delta s||_{Q_i} \end{aligned}$$

with

$$h_i(j|k) = \frac{r_i}{\eta_i}\left(\frac{2C_{d,i}}{m_i}(\Delta\bar{E}_i(j|k) + E_{i-1}^a(j|k)) + m_i g f_i\right), \tag{21}$$

$x_{des,i}(j|k) = [\delta \;\; \frac{1}{2}(m_i - m_{i-1})v_{i-1}(k)^2]^\top$ inferred from (8) and R_i, F_i, G_i, Q_i weighting matrices. More specifically, R_i is used to penalize control input error diverged from the equilibrium. F_i is used to penalize deviation between local assumed and predicted states. G_i is used to penalize output error from the desired time headway and velocity difference, and Q_i is utilized to ensure the tightness of the inequality constraint (20e), and consequently to ensure the validity of the control solution. Moreover, the dynamic system (20b) follows the nominal system (6). Conditions (20c) and (20d) are the tightened state and control constraints. The mutual inequality constraint (20e) is inherited from (2c). Finally, the problem completed by (20f), which specify the initial condition of each MPC iteration.

Overall, the distributed control algorithm can be summarized as Algorithm 1.

Algorithm 1 Tube-base Distributed MPC for a heterogeneous platoon

Offline: Determine L_i and K_i by the pole placement method, and then derive the tightened constraints via (20c) and (20d). Select suitable weighting matrices R_i, F_i, G_i, Q_i and prediction horizon N_p. At the initial position, each vehicle measures its state $x_i(0)$, and constructs the assumed trajectories $x_i^a(:|1)$ by assuming that each vehicle maintains the initial speed within a horizon window.

Online: for each vehicle $i \in \mathcal{N}$

while $k < \bar{k}$ **do**
  Call current states $x_i(k)$ and local assumed trajectories $x_i^a(:|k)$;
  Construct $\gamma_i^a(:|k)$ through $x_i^a(:|k)$;
  Receive assumed trajectories $x_{i-1}^a(:|k)$;
  Calculate optimization problem (20);
  Obtain solutions $x_i^*(:|k)$ and $u_i^*(:|k)$;
  Generate $x_i^a(:|k+1)$ based on $x_i^*(:|k)$ (see Fig.2);
  Implement the optimal input $u_i^*(1|k)$ to the real system (4);
  Measure states $x_i(k+1)$;
  $k \leftarrow k+1$;
end while

IV. Simulation Results

Numerical simulation results are given in this section. A heterogeneous platoon combined with one leader and four follower vehicles are considered. Vehicles in the platoon follow the PF communication topology. Parameters of these vehicles are shown in Table I and II, while the velocity trajectory of the leader vehicle is shown in Fig. 3. As it can be see, a time-varying velocity trajectory is considered in order to emulate the speed variation in practical dynamic traffic environment. The total simulation distance is set to 900m, which is determined by the travel distance of the leader vehicle. As it can be noticed, in this case study, we assume the heterogeneity lies in the vehicle mass, airdrag coefficient and the wheel radius whereas the tyre rolling resistance coefficient f_i, the final drive ratio η_i and state and control constraints $\mathbb{X}_i$ and $\mathbb{U}_i$ are the same for all vehicles in the platoon. More specifically, $\Delta t_i \in [0.2, 2]$ s, $\Delta E_i \in [-30, 40]$ kJ, and $T_i \in [-250, 300]$ Nm. Tightened feasible sets (see Section III-A) are solved by Multi-Parametric Toolbox 3 [26]. The obtained tightened bounds for Δt_i and ΔE_i and T_i are $[0.213, 1.987]$ s, $[-28.59, 38.59]$ kJ, $[-97.559, 147.560]$ Nm, respectively. The convex tube-based MPC is solved using the convex solver Yalmip with MOSEK [27] in Matlab environment.

TABLE I
Heterogeneity entailed in the vehicle platoon

Vehicle Index	m_i [kg]	$C_{d,i}$ [N · s^2 · m^{-2}]	r_i [m]
0	1135.7	0.39	0.30
1	1149.1	0.39	0.30
2	1234.0	0.41	0.37
3	1278.7	0.41	0.37
4	1357.6	0.43	0.39

TABLE II

OTHER PARAMETERS OF SIMULATION

Description	Symbols	Values
Tyre rolling resistance coefficient	f_i	0.01
Final drive ratio	η_i	3
Gravity constant	g	9.8 N/kg
Sampling distance interval	Δs	1 m
Desired time headway	δ	1 s

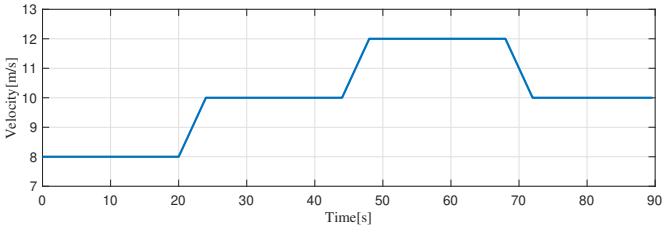

Fig. 3. Speed profile of the leader vehicle.

a) Scenario A: Let us first consider a noise-free case where $d_i(t) = 0$ and $w_i(t) = 0$. Initial conditions of the platoon system (4) is given in Table III, which do not necessarily meet the consensus requirements. The behavior of the distributed MPC control platoon is illustrated in Figs. 4 and 5.

TABLE III

VEHICLES DYNAMIC STATES AT THE INITIAL POSITION

Vehicle Index	Initial time $t_i(0)$ [s]	Initial speed $v_i(0)$ [m/s]
0	0	8
1	1.5	10
2	2	10
3	3.5	10
4	4	10

As it can be seen, the platoon system can reach preset objectives (7a) and (7b) in such a condition with all following vehicles driving at the speed equal to the leader and maintaining a constant time headway between consecutive vehicles.

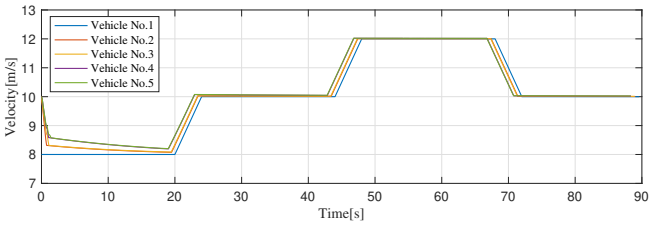

Fig. 4. Speed profiles of vehicles in the platoon in absence of disturbances.

b) Scenario B: Now, we show the algorithm is valid also in presence of the disturbances. Consider 2% process disturbances and 2% measurement noises on both time and velocity. The initial conditions of the system are the same as used in Scenario A.

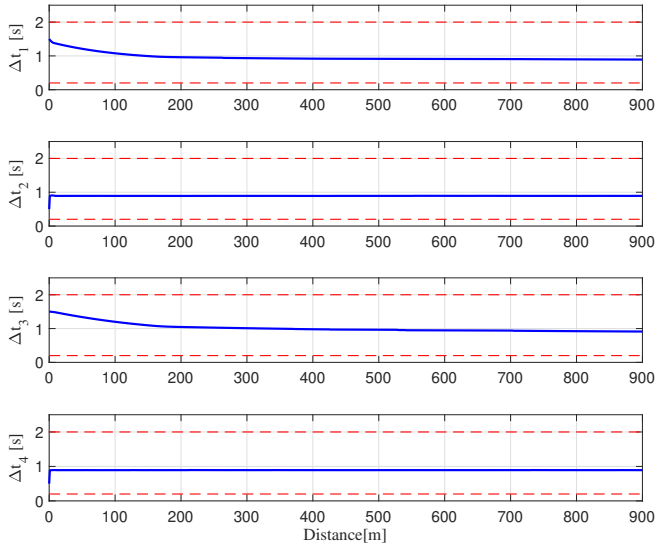

Fig. 5. The time gap between adjacent vehicles in absence of disturbances.

From the results shown in Fig. 6 and Fig. 7, both the velocities and time headways tracking errors are bounded around the equilibrium, which verifies the effectiveness of the tube-based MPC algorithm.

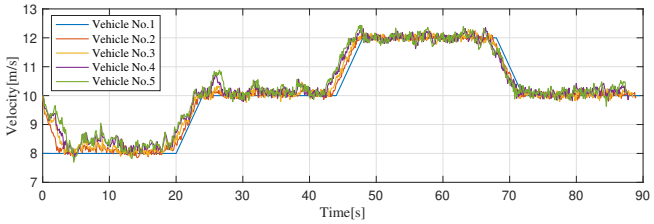

Fig. 6. Speed profiles of each vehicles in the platoon in the presence of process and measurement disturbances.

Finally, to verify the validity of this algorithm, we need to ensure $\zeta_i(k)$ equals to $\frac{1}{\sqrt{2E_i(k)/m_i}}, \forall i$ throughout the simulation. This can be achieved by increasing the weight coefficient Q_i. This has been verified in Fig. 8, and therefore it implies the validity of the control solution.

V. CONCLUSION AND FUTURE WORK

In this work, we propose a distributed robust control framework for heterogeneous vehicle platoons under PF communication topology. Under the proposed MPC framework, the platoon system is modeled in the space domain with respect to the time and kinetic energy differences. As such, a convex framework can be proposed, which enhances computational efficiency compared to nonlinear optimization approaches that appear in the literature. Both process and measurement disturbances are addressed in the paper using a tube-based MPC algorithm, which turns out to be useful in practice. Simulation examples confirm the effectiveness of the proposed method.

Future work consists in addressing communication delays and packet loss that appear in a networked control system will be addressed.

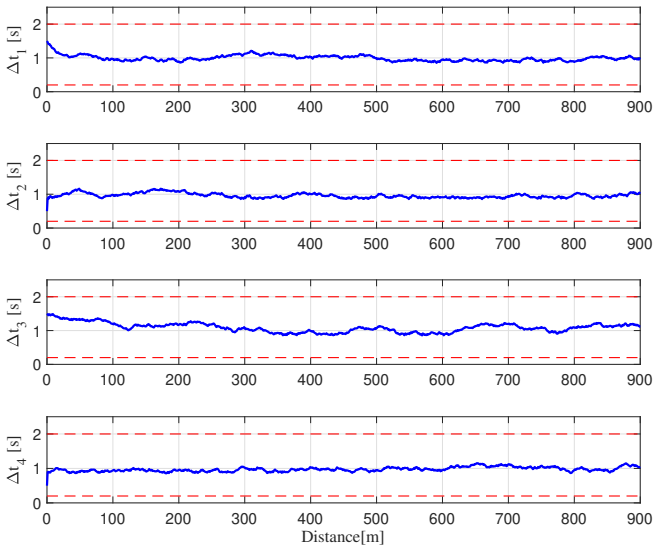

Fig. 7. The time gap between adjacent vehicles in the presence of process and measurement disturbances.

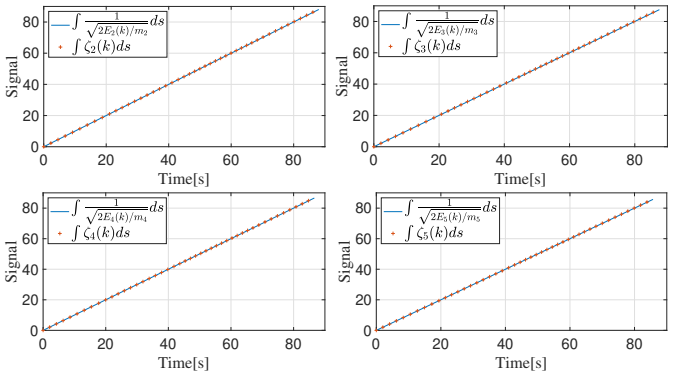

Fig. 8. The integration of $\zeta_i(k)$ and $1/\sqrt{2E_i(k)/m_i}$. The coincidence of both verifies the validity of the control solution.

REFERENCES

[1] S. Shladover, C. Desoer, J. Hedrick, M. Tomizuka, J. Walrand, W.-B. Zhang, D. McMahon, H. Peng, S. Sheikholeslam, and N. McKeown, "Automated vehicle control developments in the path program," *IEEE Transactions on Vehicular Technology*, vol. 40, no. 1, pp. 114–130, 1991.

[2] T. Robinson, E. Chan, and E. Coelingh, "Operating platoons on public motorways: An introduction to the sartre platooning programme," in *17th world congress on intelligent transport systems*, vol. 1, 2010, p. 12.

[3] L. Kahaner, "Platooning is closer than you think–just like the trucks," 2015.

[4] K.-Y. Liang, J. Mårtensson, and K. H. Johansson, "Heavy-duty vehicle platoon formation for fuel efficiency," *IEEE Transactions on Intelligent Transportation Systems*, vol. 17, no. 4, pp. 1051–1061, 2015.

[5] Y. Li, Z. Zhong, Y. Song, Q. Sun, H. Sun, S. Hu, and Y. Wang, "Longitudinal platoon control of connected vehicles: Analysis and verification," *IEEE Transactions on Intelligent Transportation Systems*, 2020.

[6] Y. Zhu and F. Zhu, "Distributed adaptive longitudinal control for uncertain third-order vehicle platoon in a networked environment," *IEEE Transactions on Vehicular Technology*, vol. 67, no. 10, pp. 9183–9197, 2018.

[7] F. Dong, X. Zhao, and Y.-H. Chen, "Optimal longitudinal control for vehicular platoon systems: adaptiveness, determinacy, and fuzzy," *IEEE Transactions on Fuzzy Systems*, vol. 29, no. 4, pp. 889–903, 2020.

[8] C. Peng, M. M. Bonsangue, and Z. Xu, "Model checking longitudinal control in vehicle platoon systems," *IEEE Access*, vol. 7, pp. 112 015–112 025, 2019.

[9] A. Khalifa, O. Kermorgant, S. Dominguez, and P. Martinet, "Vehicles platooning in urban environment: Consensus-based longitudinal control with limited communications capabilities," in *2018 15th International Conference on Control, Automation, Robotics and Vision (ICARCV)*. IEEE, 2018, pp. 809–814.

[10] Y. Li, W. Chen, S. Peeta, and Y. Wang, "Platoon control of connected multi-vehicle systems under v2x communications: design and experiments," *IEEE Transactions on Intelligent Transportation Systems*, vol. 21, no. 5, pp. 1891–1902, 2019.

[11] Y. Zhu and F. Zhu, "Distributed adaptive longitudinal control for uncertain third-order vehicle platoon in a networked environment," *IEEE Transactions on Vehicular Technology*, vol. 67, no. 10, pp. 9183–9197, 2018.

[12] H. Wi, H. Park, and D. Hong, "Model predictive longitudinal control for heavy-duty vehicle platoon using lead vehicle pedal information," *International Journal of Automotive Technology*, vol. 21, no. 3, pp. 563–569, 2020.

[13] G. Feng, D. Dang, and Y. He, "Robust coordinated control of nonlinear heterogeneous platoon interacted by uncertain topology," *IEEE Transactions on Intelligent Transportation Systems*, 2020.

[14] H. Hao and P. Barooah, "Stability and robustness of large platoons of vehicles with double-integrator models and nearest neighbor interaction," *International Journal of Robust and Nonlinear Control*, pp. 1–26, 2012.

[15] Y. Zheng, S. E. Li, K. Li, F. Borrelli, and J. K. Hedrick, "Distributed model predictive control for heterogeneous vehicle platoons under unidirectional topologies," *IEEE Transactions on Control Systems Technology*, vol. 25, no. 3, pp. 899–910, 2017.

[16] W. B. Dunbar and D. S. Caveney, "Distributed receding horizon control of vehicle platoons: Stability and string stability," *IEEE Transactions Automatic Control*, vol. 57, no. 3, pp. 620–633, 2012.

[17] Q. Luo, A.-T. Nguyen, J. Fleming, and H. Zhang, "Unknown input observer based approach for distributed tube-based model predictive control of heterogeneous vehicle platoons," *IEEE Transactions on Vehicular Technology*, vol. 70, no. 4, pp. 2930–2944, 2021.

[18] F. Gao, S. E. Li, Y. Zheng, and D. Kum, "Robust control of heterogeneous vehicular platoon with uncertain dynamics and communication delay," *IET Intelligent Transport Systems*, vol. 10, no. 7, pp. 503–513, 2016.

[19] Y. Li, C. Tang, S. Peeta, and Y. Wang, "Nonlinear consensus-based connected vehicle platoon control incorporating car-following interactions and heterogeneous time delays," *IEEE Transactions on Intelligent Transportation Systems*, vol. 20, no. 6, pp. 2209–2219, 2018.

[20] L. Xu, W. Zhuang, G. Yin, G. Li, and C. Bian, "Simultaneous longitudinal and lateral control of vehicle platoon subject to stochastic communication delays," *Journal of Dynamic Systems, Measurement, and Control*, vol. 141, no. 4, 2019.

[21] Y. Zheng, S. E. Li, K. Li, F. Borrelli, and J. K. Hedrick, "Distributed model predictive control for heterogeneous vehicle platoons under unidirectional topologies," *IEEE Transactions on Control Systems Technology*, vol. 25, no. 3, pp. 899–910, 2016.

[22] Y. Zheng, S. E. Li, K. Li, and W. Ren, "Platooning of connected vehicles with undirected topologies: Robustness analysis and distributed h-infinity controller synthesis," *IEEE Transactions on Intelligent Transportation Systems*, vol. 19, no. 5, pp. 1353–1364, 2017.

[23] X. Pan, B. Chen, S. A. Evangelou, and S. Timotheou, "Optimal motion control for connected and automated electric vehicles at signal-free intersections," in *2020 59th IEEE Conference on Decision and Control (CDC)*. IEEE, 2020, pp. 2831–2836.

[24] D. Q. Mayne, S. V. Raković, R. Findeisen, and F. Allgöwer, "Robust output feedback model predictive control of constrained linear systems," *Automatica*, vol. 42, no. 7, pp. 1217–1222, 2006.

[25] W. Vilaivannaporn, S. Boonsith, W. Pornputtapitak, and P. Bumroongsri, "Robust output feedback predictive controller with adaptive invariant tubes and observer gains," *International Journal of Dynamics and Control*, vol. 9, no. 2, pp. 755–765, 2021.

[26] M. Herceg, M. Kvasnica, C. Jones, and M. Morari, "Multi-Parametric Toolbox 3.0," in *Proc. of the European Control Conference*, Zürich, Switzerland, July 17–19 2013, pp. 502–510.

[27] J. Löfberg, "Yalmip : A toolbox for modeling and optimization in matlab," in *Proc. of the CACSD Conference*, Taipei, Taiwan, 2004.